The Radiofrequency Spectrum of $K^{39}F$ by the Electric Resonance Method*

LUDWIG GRABNER** AND VERNON HUGHES
Columbia University, New York, New York

(Received February 24, 1950)

The molecular beam electric resonance method has been used to investigate the rotational Stark spectrum of $K^{39}F$. In this method linear polar diatomic molecules in one, or at most two, rotational states and definite states of space quantization are selected by means of inhomogeneous electric fields. The molecular transitions are not of the ΔJ type (transition between different rotational states). Rather, the transitions are between states with the same value of J but different values of m_J, the electric quantum number characterizing the state of space quantization. Lines are observed as a change in intensity of the refocused beam when the frequency of an oscillating field, which is perpendicular to an homogeneous field, times Planck's constant is equal to the energy difference between different states of space quantization. The frequency of the rotational Stark line is determined by the value of the homogeneous static field. The Stark line was observed at low and high fields for $J=1$ and low fields for $J=2$. It is found to be split. The fine structure is due to an interaction of the nuclear electric quadrupole moment of the K^{39} nucleus with the rest of the charges of the molecule as well as a variation of $\mu^2 A$ with the vibrational state of the molecule. Here μ is the permanent electric dipole moment, and A is the moment of inertia. In addition, the quadrupole interaction constant is found to vary with the vibrational state. It is measured when the molecule is in the rotational state $J=1$ and the vibrational states $v=0$, 1, 2, 3 and 4; and $J=2$, $v=0$, 1 and 2.

The frequency dependence of the Stark line at strong fields permits the determination of μ and A; they were determined only for the zeroth vibrational state.

The results are: For $J=1$, $v=0$, $eqQ/h=(-7.938\pm0.040)$ Mc/sec. The absolute value of eqQ/h decreases about 1.3 percent when the vibrational quantum number increases by unity. Within experimental error the quadrupole interaction and its variation with vibrational state for $J=2$ is the same as for $J=1$. A complete tabulation of the results will be found in Table II. For the zeroth vibrational state $\mu=(7.33\pm0.24)$ Debye, $A=(138.4\pm6.9)\times10^{-40}$ g-cm^2. From A we find for the internuclear distance for the zeroth vibrational state $r=(2.55\pm0.06)$ angströms. From the variation in intensity with vibrational state for a single transition the vibrational constant $\omega_0=(390\pm39)$ cm^{-1}.

I. INTRODUCTION

THE electric resonance method[1–3] of molecular beams has one important feature which distinguishes it from the magnetic resonance method[4] in the investigation of the hyperfine structures of linear polar diatomic molecules. It is able to select for investigation a single rotational state of such a molecule. In the magnetic resonance method all of the rotational states are refocused, because a magnetic field is used. If the interactions causing the spectrum depend on the rotational state, the spectrum will be a superposition of those of all of the rotational states, and therefore will be of statistical character. The spectra observed in the electric resonance method are "pure," in the sense that they are caused by a single rotational state. Thus fine details are recorded in the simplest way and are not obscured by the presence of many rotational states. Therefore the interpretation is easier and the data more accurate.

The important disadvantage of the electric relative to the magnetic resonance method is that it is confined to molecular spectroscopy and even in that field can handle only polar molecules. Moreover, the method has thus far been worked out only for diatomic molecules. The magnetic resonance method is inherently free from these limitations. A nuclear g-value can, of course, only be measured by the magnetic resonance method; an electric dipole moment or a moment of inertia only by the electric resonance method. Quadrupole and $\mathbf{I}\cdot\mathbf{J}$ interactions[5,6] can be determined by both methods[2,7,8] if the molecule is a polar diatomic molecule.

II. EXPERIMENTAL

The apparatus used in this experiment is the one built by Hughes,[1] with the C-field modified by Trischka,[2] and has been described in detail by them. It is shown schematically in Fig. 1 of reference 1.

A refocused beam of molecules of a fixed rotational state J can be obtained in two distinct ways. This will be illustrated for the rotational state $J=1$. Figure 1 shows μ_e/μ as a function of $\lambda=\mu E/(\hbar^2/2A)$, a dimensionless parameter characterizing the value of the field, for various J, m_J states of a linear polar diatomic molecule. Here μ is the permanent, μ_e the effective electric dipole moment, A is the moment of inertia, E is the value of the electric field, m_J is the electric quantum number characterizing the state of space quantization. If the A and B fields are set at a λ value of $\lambda_A{}^{1,0}$ and $\lambda_B{}^{1,0}$, respectively (see Fig. 1), then, for the apparatus used in this experiment, a molecule in the 1, 0 state will suffer equal and opposite deflections in the A and B fields, assuming the directions of field and gradient of the field to be that shown in Fig. 1 of reference 1, and can be refocused on a suitably aligned detector. The values $\lambda_A{}^{1,0}$ and $\lambda_B{}^{1,0}$ shown in Fig. 1 were chosen be-

* This research has been supported in part by the ONR.

** Submitted by Ludwig Grabner in partial fulfillment of the requirements for the degree of Doctor of Philosophy in Physics at Columbia University.

[1] H. K. Hughes, Phys. Rev. **72**, 614 (1947).
[2] J. W. Trischka, Phys. Rev. **74**, 718 (1948).
[3] J. W. Trischka, Phys. Rev. **76**, 1365 (1949).
[4] Rabi, Millman, Kusch, and Zacharias, Phys. Rev. **55**, 526 (1939).
[5] H. M. Foley, Phys. Rev. **72**, 504 (1947).
[6] G. C. Wick, Phys. Rev. **73**, 51 (1948).
[7] W. A. Nierenberg and N. F. Ramsey, Phys. Rev. **72**, 1075 (1947).
[8] V. Hughes and L. Grabner, Phys. Rev. **79**, 314 (1950).

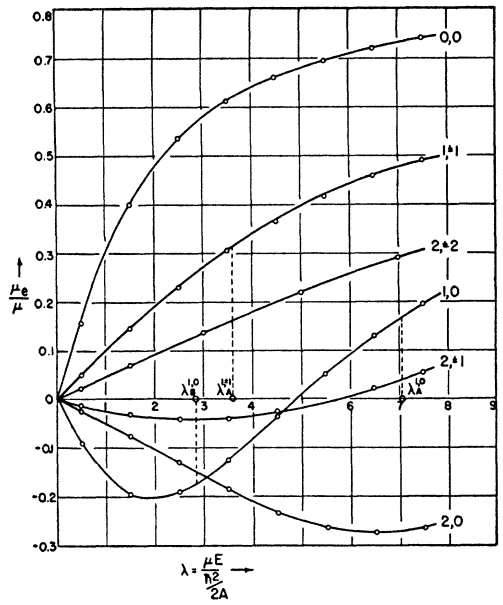

FIG. 1. Effective electric moments of a rotating polar diatomic molecule in an electric field.

cause they give a maximum deflection at the wire stop. A beam refocused in this way will be designated as a $(1, 0)_A-(1, 0)_B$ beam because the molecules that are refocused are in the state 1, 0 in both the A and B fields. There is, however, another way of refocusing molecules in the rotational state $J=1$. Since the magnitude and direction of the electric field change in the interfield regions, it is possible for a molecule to change its state of space quantization because of its passage through such a region. These non-adiabatic transitions can be used in the following way to refocus molecules in the rotational state $J=1$. If the B-field is left at its previous value $\lambda_B{}^{1,0}$ while the A-field is changed to $\lambda_A{}^{1,\pm1}$, shown in Fig. 1, a molecule in the $1, \pm1$ state will suffer the same deflection as a molecule in the 1, 0 state did when the A-field was $\lambda_A{}^{1,0}$. Non-adiabatic transitions from the $1, \pm1$ state to the 1, 0 state in the regions between the A and C fields and between the C and B fields will cause 1, 0 molecules of the proper deflection to enter the B-field. These are then refocused on the detector. A refocused beam obtained in this way will be designated as a $(1, \pm1)_A-(1, 0)_B$ beam because the molecules that are refocused are in the $1, \pm1$ state in the A-field and in the 1, 0 state in the B-field. Presumably most of the non-adiabatic transitions occur between the A and C fields since the collimator slit is placed there and causes larger variations of the field than there are between the C and B fields. Which type of refocused beam is chosen for experimentation is decided by which gives the greater intensity of transitions. Theoretically both are valid and give the same results.

A total beam of 500,000 cm measured on a galvanometer scale was used and stopped down by means of the wire stop to 20 cm. The refocusing conditions were such that the intensity of the refocused beam was 50 cm. For the moderately strong and strong field experiments the $(1, 0)_A-(1, 0)_B$ refocused beam was used. For the weak field experiments the $(1, \pm1)_A-(1, 0)_B$ refocused beam was used. The isotopes K^{39} and K^{41} are present in the refocused beam with percentages of 93.44 and

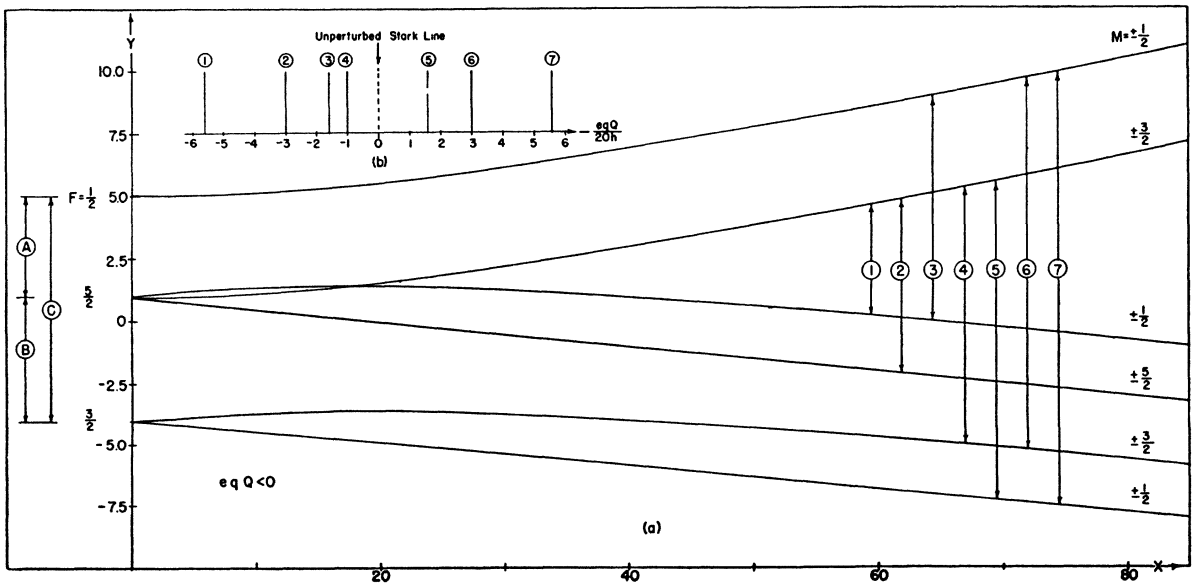

FIG. 2. (a) Plot of energy levels W *versus* the square of the electric field, E^2, for $J=1$, $I=\frac{3}{2}$ and $eqQ<0$; coordinates are in dimensionless units.

$$Y=-20\frac{W}{eqQ} \qquad X=-20\frac{(\mu E)^2}{eqQ(h^2/2A)}$$

(b) Strong field spectrum for $J=1$, $I=\frac{3}{2}$, $eqQ<0$.

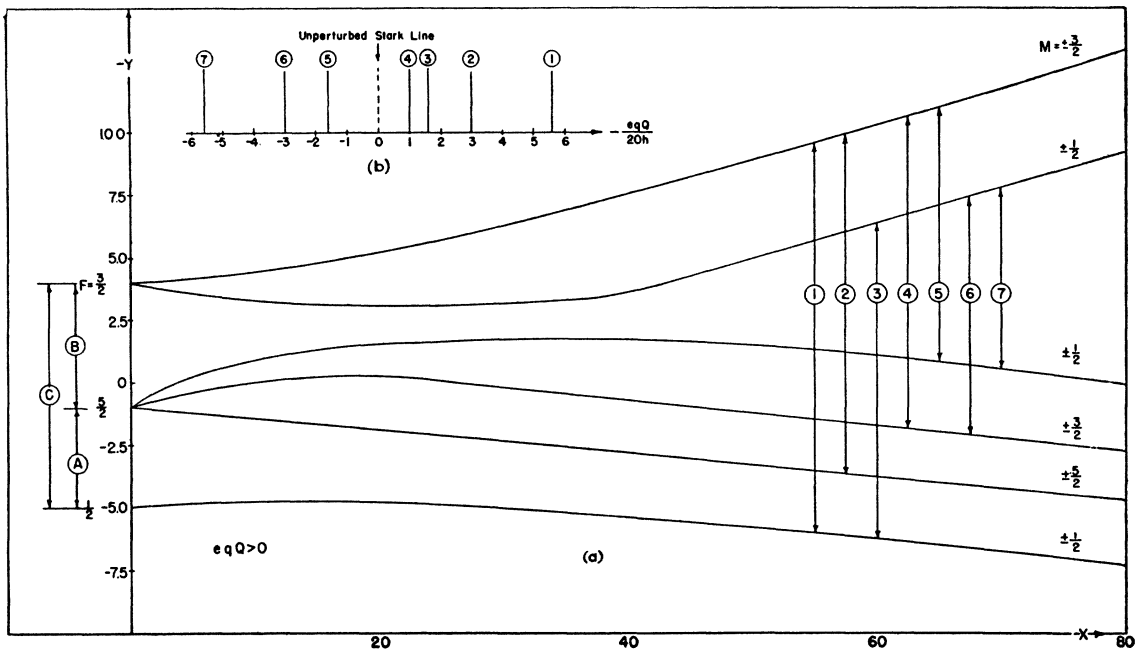

FIG. 3. (a)Plot of energy levels W *versus* the square of the electric field, E^2, for $J=1$, $I=\frac{3}{2}$ and $eqQ>0$; coordinates are in dimensionless units.

$$Y=-20\frac{W}{eqQ} \qquad X=-20\frac{(\mu E)^2}{eqQ(h^2/2A)}$$

(b) Strong field spectrum for $J=1$, $I=\frac{3}{2}$, $eqQ>0$.

6.55 percent, respectively. The r-f field induces transitions causing a maximum change of refocused beam intensity of 6 to 7 cm. Detector and beam stability were such that under best conditions a change of 5 mm in the refocused beam could be observed. Because of insufficient abundance the spectrum of $K^{41}F$ could not be observed.

III. THEORY

The results of the experiment can be interpreted by assuming the following Hamiltonian[9–11]

$$H=\frac{h^2}{2A}\mathbf{J}^2-\boldsymbol{\mu}\cdot\mathbf{E}-eqQ\frac{\{3(\mathbf{I}\cdot\mathbf{J})^2+\frac{3}{2}(\mathbf{I}\cdot\mathbf{J})-\mathbf{I}^2\mathbf{J}^2\}}{2I(2I-1)(2J-1)(2J+3)}. \quad (1)$$

In the first term $\mathbf{J}$ is the angular momentum of rotation of the molecule and A is the moment of inertia. The second term represents the interaction of the field with the permanent dipole moment of the molecule. The third term represents the electric quadrupole interaction of the K^{39} nucleus with the rest of the charges of the molecule. e=the charge of the proton, Q=nuclear electric quadrupole moment, $q=\partial^2V/\partial z^2$ the second derivative of the electrostatic potential due to all the charges outside the nucleus, taken along the axis of the molecule at the position of the nucleus.[12] The quantity I is the spin of the K^{39} nucleus. The fluorine

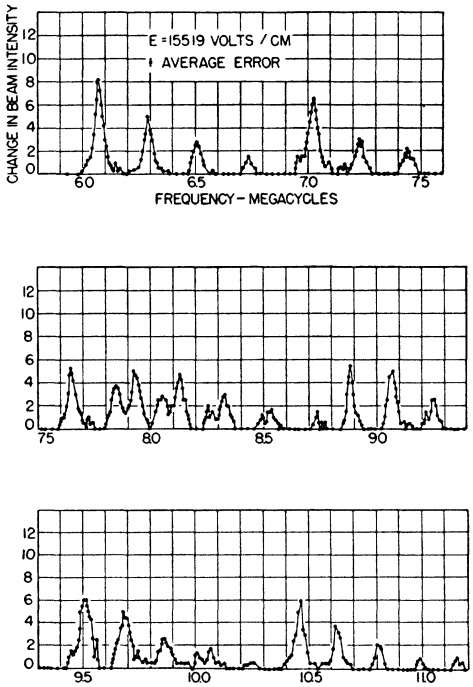

FIG. 4. Moderately strong field spectrum. This spectrum is drawn schematically in Fig. 5, where the lines are identified.

[9] U. Fano, J. Research Nat. Bur. Stand. **40** (1948) Research Paper 1866.
[10] Nierenberg, Rabi, and Slotnick, Phys. Rev. **73**, 1430 (1948).
[11] V. Hughes and L. Grabner (to be published).
[12] J. Bardeen and C. H. Townes, Phys. Rev. **73**, 97 (1948).

nucleus with a spin of $\frac{1}{2}$ has no quadrupole interaction. The theory of Fano[13] was used to calculate the energy level diagram shown in Fig. 2a when $eqQ<0$, $J=1$ and $I=\frac{3}{2}$. In calculating the energy levels the influence of the mixing of the J states on the matrix elements of the quadrupole interaction can be neglected.

At zero field $\mathbf{I}$ couples to $\mathbf{J}$ through the quadrupole interaction to split the rotational energy level $J=1$ into three levels labeled by the quantum numbers $F=I+J$ as 1/2, 3/2 and 5/2. At weak fields, defined by $|eqQ| \gg \mu^2E^2/(\hbar^2/2A)$ each zero field level splits into $1/2(2F+1)$ levels and each energy level is characterized by F and its projection m_F. Because the field is electric, states with the same value of F differing only in the sign of m_F are degenerate. As the field is increased $\mathbf{I}$ and $\mathbf{J}$ decouple until at strong fields (i.e., when $|eqQ| \ll \mu^2E^2/(\hbar^2/2A)$) the (J, m_J) states $(1, \pm 1)$ and $(1, 0)$, which at low and intermediate fields are mixed by the quadrupole interaction, separate. Because of the quadrupole interaction the $(1, 0)$ level is split into two energy levels which increase in energy as the field is increased. The $(1, \pm 1)$ level is split into four energy levels which decrease in energy as the field is increased. Each of the terms in Eq. (1) may depend on the vibrational state, so that Fig. 2a must be considered as the energy level diagram when the molecule is in a certain vibrational state characterized by the vibrational quantum number v. The selection rule[14] for transitions as strong fields is $\Delta(m_J+m_I) \equiv \Delta M = 0, \pm 1$. This gives rise to seven lines labeled numerically in Fig. 2a. At strong fields the relative positions of these lines with respect to the unperturbed Stark line is independent of the field, and is shown in Fig. 2b. The unperturbed Stark line is the single line that would be observed if there were no quadrupole interaction and no variation of the $\boldsymbol{\mu}\cdot\mathbf{E}$ interaction with vibrational state. In that case the 1, 0 and 1, ± 1 levels are not split. If the $\boldsymbol{\mu}\cdot\mathbf{E}$ and quadrupole interaction vary with the vibrational state, the spectrum is a superposition of the spectra of all the vibrational states. The vibrational states are identified by the intensities of the lines. The intensities decrease as $\exp(-E_v/kT)$, E_v is the energy of the vibrational state v, k is the Boltzmann constant, and T is the absolute temperature of the oven. At weak fields the selection rules are $\Delta F = 0, \pm 1, \pm 2$ and $\Delta m_F \equiv \Delta M = 0, \pm 1$. This gives rise to three lines which are identified by the letters A, B and C in Fig. 2a. At weak fields the $\boldsymbol{\mu}\cdot\mathbf{E}$ interaction is very small. Lines arising from transitions between different m_F levels into which each F level splits at weak fields were not resolved in the low field runs of this experiment. If the quadrupole interaction varies with the vibrational state, the spectrum again will be a superposition of those of all the vibrational states with an intensity distribution characterized by $\exp(-E_v/kT)$. Transitions within a rotational state are forbidden at zero field.

The r-f field causing the transitions is arranged so that if it is decomposed into components parallel and perpendicular to the steady field, $E_{\mathrm{rf}\perp} > E_{\mathrm{rf}\parallel}$; $E_{\mathrm{rf}\perp}$ gives rise to transitions for which $\Delta M = \pm 1$, $E_{\mathrm{rf}\parallel}$ to those for which $\Delta M = 0$.

If $eqQ>0$ the energy level diagram is different and is sketched in Fig. 3a. The strong field spectrum is shown in Fig. 3b. The transitions in Fig. 3b are labeled in such a way that a transition between two levels has the same label as the corresponding transition has in Fig. 2a. The strong field spectrum shown in Fig. 3b is identical with that shown in Fig. 2b except for the position of

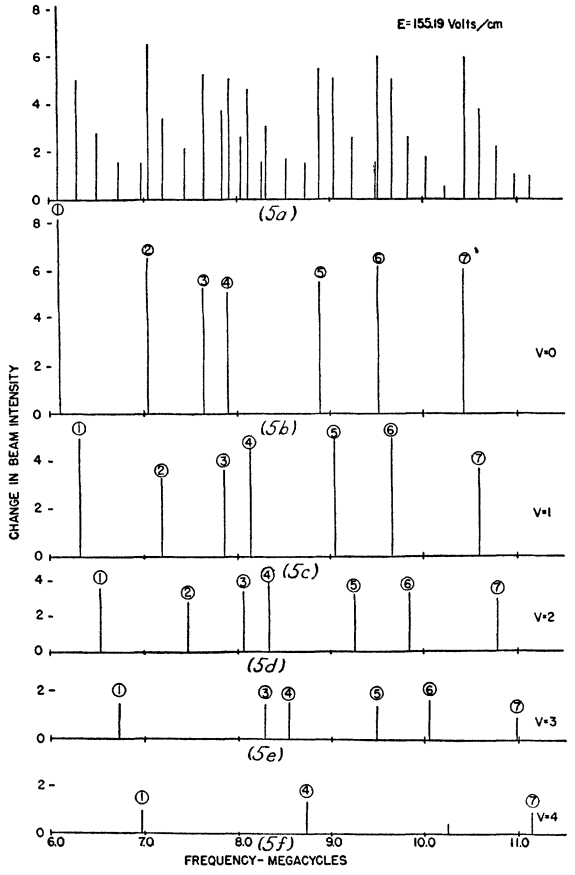

FIG. 5. (a) Moderately strong field spectrum of $K^{39}F$ (schematic). (b), (c), (d), (e), and (f) are the vibrational states $v=0$, 1, 2, 3, 4 as analyzed from (a).

[13] See reference 9. Fano's definition of q differs from that used in this paper. Note also that in the initial report of this research in the abstracts of the June 1949 American Physical Society meeting at Cambridge, q' rather than q was used. Since our first report it has been agreed in this laboratory in the interest of uniformity to use q as defined by Bardeen and Townes. B. T. Feld and W. E. Lamb, Phys. Rev. **67**, 15 (1948), use a definition of q which differs from Fano's q, q', and from the q of Bardeen and Townes. The relationship between these q's is:

$$q_{\text{Bardeen-Townes}} = 2eq' = -eq_{\text{Fano}} = -2eq_{\text{Feld-Lamb}}(2J+3)/2J$$

e = proton charge, J = rotational quantum number. The advantage of $q_{\text{Bardeen-Townes}}$ is that it directly represents $\partial^2V/\partial z^2$ at the nucleus along the molecular axis and not a quantity which when multiplied by a suitable factor gives $\partial^2V/\partial z^2$.

[14] The selection rules are treated in detail in reference 11.

TABLE I. Comparison of observed and predicted lines. Lines are identified in Fig. 2. Lines 2, 3, 4, 5, 6; eqQ/h, μ^2A were calculated from lines 1 and 2.

Vibrational state ↓	Line→	(1)	(2)	(3)	(4)	(5)	(6)	(7)	$-(eqQ/h)$ Mc/sec.	$\mu^2A \times 10^{-76}$ e.s.u.
0	observed (Mc)	6.070	7.028	7.645	7.930	8.883	10.461	7.645	7.928	7419.3
	predicted		7.024	7.647	7.938	8.884	10.461			
1	observed	6.286	7.218	7.846	8.127	9.062	9.682	10.617	7.816	7598.1
	predicted		7.230	7.842	8.126	9.062	9.681			
2	observed	6.507	7.440	8.047	8.327	9.250	9.857	10.800	7.744	7789.4
	predicted		7.444	8.048	8.328	9.259	9.870			
3	observed	6.735		8.276	8.535	9.445	10.068	10.988	7.668	7986.4
	predicted		7.666	8.262	8.537	9.461	10.064			
4	observed	6.953			8.736		10.250	11.150	7.566	8166.6
	predicted		7.873	8.458	8.729	9.643	10.235			

line 4. If $eqQ>0$ line 4 lies to the right, if $eqQ<0$ to the left of the unperturbed Stark line. Thus a strong field spectrum not only determines the magnitude of the quadrupole interaction but the sign as well because of the asymmetry introduced by line 4.

It will now be shown that a weak field spectrum also allows the determination of the sign of eqQ even though the weak field spectrum is independent of the sign. This is possible because of the way in which a line is observed in a molecular beam experiment. Clearly a transition is observable only if it occurs between a state that is refocused and one that is not; i.e., it must be a transition between states that may be adiabatically transformed into levels that differ in the value of $|m_J|$. Regardless of whether the $(1,0)_A-(1,0)_B$ or the $(1,\pm1)_A-(1,0)_B$ beam is refocused it is evident from Fig. 2a and 3a that lines B and C will be observed irrespective of the sign of the quadrupole interaction but that line A will be observed only if $eqQ<0$ because only in this case can the states between which transition A takes place be adiabatically transformed into states that differ in $|m_J|$. Therefore the appearance or absence of line A also decides the sign of the quadrupole interaction.

IV. THE SPECTRA

Figure 4 shows the spectrum obtained at a moderately strong field. The spectrum was observed by fixing the C-field at 155.19 volts/cm and varying the frequency. The lines are due to a quadrupole interaction with the K^{39} nucleus and a variation of the $\boldsymbol{\mu}\cdot\mathbf{E}$ interaction with vibrational state. In addition, it will be shown that the spectrum shows a variation of the quadrupole interaction with vibrational state. The value of the electric field is such that the splitting of the unperturbed Stark line due to the quadrupole interaction is not quite yet independent of the field; i.e., the spectrum is not a true strong field spectrum. Each transition occurs within all the vibrational states and its frequency relative to the unperturbed Stark line is determined, at this moderately strong field, principally by the quadrupole interaction. The unperturbed Stark line is determined by the $\boldsymbol{\mu}\cdot\mathbf{E}$ interaction. Since many more than the predicted seven lines are observed it is clear that the $\boldsymbol{\mu}\cdot\mathbf{E}$ interaction varies with vibrational state and that the magnitude of this effect is large enough to resolve the vibrational states of the molecule. In the center of the spectrum some of the transitions almost overlap. For clarity, therefore, the spectrum shown in Fig. 4 was plotted schematically in Fig. 5a. The positions and lengths of the lines in Fig. 5a are drawn at the frequency and equal to the intensity at which they were observed. The spectra of molecules in the vibrational states $v=0$, 1, 2, 3 and 4 were selected from Fig. 5a and redrawn separately in Fig. 5b, c, d, e and f, respectively. In the vibrational states $v=3$ and 4 not all the lines are resolved. The lines are labeled by numbers in Fig. 5 and the transition to which each

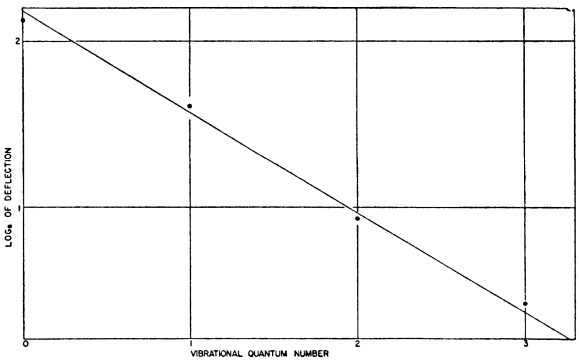

FIG. 6. Semi-log plot of the intensity of line 1, identified in Fig. 2, *versus* vibrational quantum number. Oven temperature 920°K. $\omega_0=(390\pm39)$ cm^{-1}.

corresponds is identified by the corresponding number in Fig. 2a. The spectrum was obtained from several different runs. Conditions determining the intensity of a line were not the same in the different runs. This is shown in the intensities of the different vibrational states which theoretically should be homologous. The identification of the vibrational state and, in fact, the principal reason for regarding these lines as transitions within several vibrational states is the variation of intensity of a single transition with vibrational state. The population of a vibrational state and therefore the intensity of its corresponding line goes as $\exp(-E_v/kT)$. If the natural logarithm of the intensity of a line is plotted as a function of the vibrational state a straight line should result. This is borne out particularly well by line 1, as is shown in Fig. 6. From the line intensities for the different vibrational states and the oven temperature[15] $\omega_0=(390\pm39)$ cm^{-1}. Inclusive of the $\Delta M=0$ transition, the theory predicts seven lines. All of these are observed. Several are missing for the

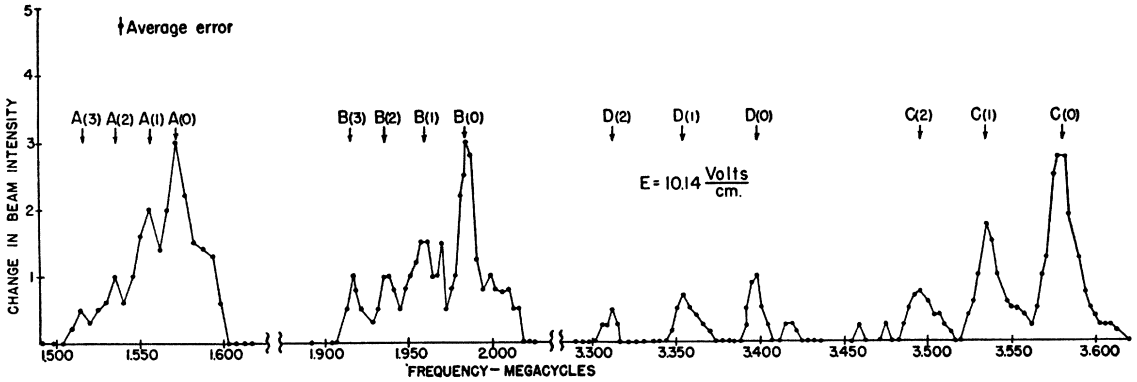

FIG. 7. Weak field spectrum. Lines are identified in Fig. 2. Vibrational states are identified by vibrational quantum numbers attached to letters as subscripts.

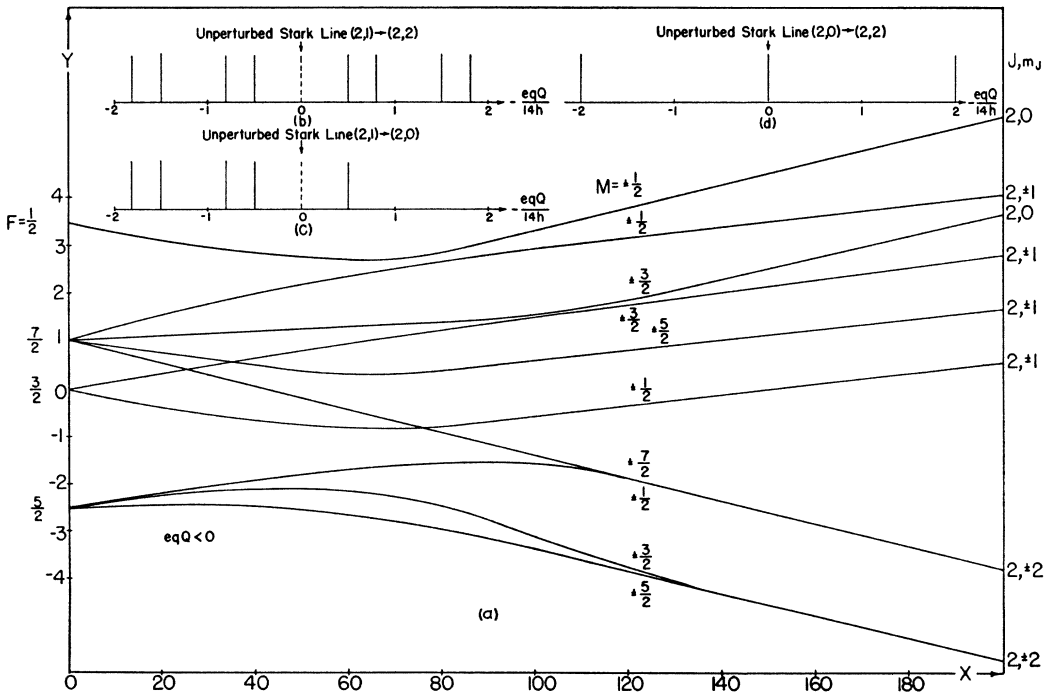

FIG. 8. (a) Plot of energy levels W *versus* the square of the electric field, E^2, for $J=2$, $I=\frac{3}{2}$, $eqQ<0$; coordinates are in dimensionless units.

$$Y=-14\frac{W}{eqQ} \qquad X=-14\frac{(\mu E)^2}{eqQ(h^2/2A)}$$

(b), (c), and (d), strong field spectrum for $(J, m_J)\rightarrow(J, m_J')$ of (2, 1)→(2, 2); (2, 0)→(2, 1); and (2, 0)→(2, 2), respectively.

[15] G. Herzberg, *Molecular Spectra and Molecular Structure, I. Diatomic Molecules* (Prentice-Hall, Inc., New York, 1939), p. 101.

TABLE II. Quadrupole interaction constant eqQ/h for K^{39} in $K^{39}F$ for the vibrational states $v=0, 1, 2, 3, 4$ in rotational state $J=1$ and for vibrational states $v=0, 1, 2$ with rotational state $J=2$.

Rotational state J	Vibrational state V	"Strong" field $-(eqQ/h)$ Mc/sec.	Weak field $-(eqQ/h)$ Mc/sec. From line (A)	From line (B)	From line (C)	Average weak field data	Difference between "strong" and weak	Average of strong and weak field data $-(eqQ/h)$ Mc/sec.
	0	7.928	7.952	7.968	7.906	7.946	0.018	7.938±0.040
	1	7.816	7.856	7.842	7.828	7.842	0.026	7.828±0.040
1	2	7.744	7.766	7.742	7.724	7.744	0.000	7.744±0.040
	3	7.668	7.676	7.646	7.620	7.648	0.020	7.658±0.040
	4	7.566						
			From line (D)					
	0		7.928±0.040					
2	1		7.828±0.040					
	2		7.726±0.040					

vibrational state $v=3$ and 4 (see Fig. 5e and 5f) because they fell within the line width of lines in lower vibrational states and thus were not resolved. The resolution is determined by three factors.[16] (1) The inhomogeneity of the C-field sets a limit of 1 part in 1000 of the frequency, i.e., 18 kc/sec. (2) The uncertainty relation $\Delta\nu\Delta t\sim 1$ where $h\Delta\nu$ is the uncertainty in the energy, and Δt is the time the molecule spends in the oscillating field, results in a broadening of 16 kc/sec. for KF at an oven temperature of 650°C and for an effective length of the C-field of 4 cm. (3) The magnitude of the oscillating field. The theoretical width resulting from a combination of the first two estimates was not calculated. The half-width of the lines in Fig. 4 is 40 kc/sec. Subsequent experiments showed that the r-f voltage $=0.75$ r.m.s. volts was too large by a factor of about 10 and that a correct r-f field would have narrowed the lines to $\sim$20 kc/sec.

The arithmetic mean of the frequencies of lines 1 and 7 give to a good approximation the frequency of the unperturbed Stark line, which is proportional to μ^2AE^2 at this moderately strong field.[17] Since the position of line 4 is to the left of the unperturbed Stark line $eqQ<0$ (see Figs. 2 and 3).

Taking into account the fact that Fig. 4 does not represent a strong field spectrum μ^2A and eqQ were calculated for each vibrational state. Any two lines in a given vibrational state determine μ^2A and eqQ for that vibrational state. From these two constants the consistency of the theory and the data can be checked by predicting the frequencies of the other lines and comparing these frequencies with those found in the experiment. Table I shows the results of such a calculation using lines 1 and 7 to calculate μ^2A, eqQ, and the positions of the other lines. Evidently the agreement between the predicted frequencies and those found experimentally is excellent. It is also significant that this moderately strong field experiment reveals a decrease in the magnitude of the quadrupole interaction as the vibrational quantum number increases, of approximately 1.3 percent when the vibrational quantum number increases by unity.

Structure at Weak Fields

At weak fields the $\boldsymbol{\mu}\cdot\mathbf{E}$ interaction is small compared with the quadrupole interaction. In particular, if the quadrupole interaction is not a function of the vibrational state, the lines that occur because $\boldsymbol{\mu}\cdot\mathbf{E}$ is a function of the vibrational state would not be resolved at the low fields used in this experiment. At weak fields the resolution is determined by the uncertainty relation, and is 16 kc/sec. Since the effect of the field on the spectrum is practically eliminated, it will exhibit primarily internal interactions. A variation of the quadrupole interaction is anticipated from the moderately strong field spectrum. A calculation of the effect of such a variation on a weak field spectrum shows that a single transition occurring in different vibrational states should be resolved. The effect of the field is to split the zero field energy levels as shown in Fig. 2a. The resultant splitting of the lines is of the same order of magnitude as the resolution, and is not expected to be resolved. Since $eqQ<0$, as determined from the moderately strong field experiment, the theory predicts three lines according to the selection rules $\Delta F=0, \pm1, \pm2$; $\Delta m_F=0, \pm1$. These transitions are labeled in the energy level diagram, Fig. 2a, as lines A, B and C. Figure 7 shows the data obtained at a

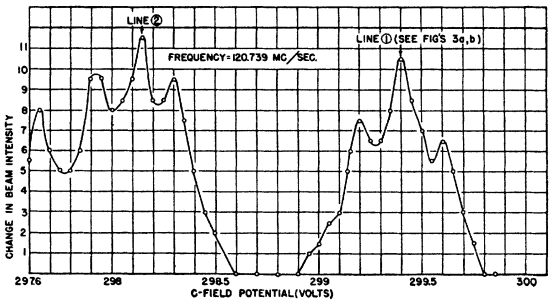

FIG. 9. Strong field spectrum showing the 0th vibrational state of lines 1 and 2 (see Fig. 2a,b) and the side peaks of lines 1 and 2 produced by the Millman effect. Peak at $V_c=297.65$ volts belongs to another line.

[16] See reference 2, p. 720.

[17] P. Debye, *Polar Molecules* (Dover Publications, New York, 1945).

C-field of 10.14 volts/cm. The lines are labeled by letters in Fig. 7 and the transition to which each corresponds is identified by the corresponding letter in Fig. 2a. The vibrational state within which the transition takes place is identified by the vibrational quantum number attached as a subscript. Since line A appears in the spectrum, $eqQ<0$, in agreement with the moderately strong field spectrum. The assignment of the lines is correct because their frequency ratios agree with the theory.

Line D (see Fig. 7) cannot be explained as arising from a transition in the energy level diagram of Fig. 2a. All possible transitions have already been exhausted by lines A, B, and C. Furthermore, it is impossible that it could be due to the effect of the field since any splitting of the lines caused by the field is far too small to account for it. An inspection of the energy level diagram corresponding to Fig. 2a for the rotational state $J=2$ shows that line D comes from a transition in which F changes from $5/2\rightarrow1/2$, the latter states arising from a perturbation of the rotational states $J=2$ by the quadrupole interaction. The energy level diagram for $J=2$, $I=3/2$, $eqQ<0$ is sketched in Fig. 8a. Two considerations support this conclusion. (1) The weak field data were obtained with the $(1,\pm1)_A-(1,0)_B$ refocused beam. The A and B fields required to refocus this beam will also refocus some of the $(2,\pm2)_A-(2,0)_B$ beam since not all of its molecules are eliminated by the wire stop. (2) If we assume that eqQ does not change with rotational state, the value of the quadrupole interaction calculated from the moderately strong field data or from the weak field lines A, B or C predicts a line exactly where line D occurs caused by the transition $F=1/2\rightarrow5/2$ within the energy levels of the rotational state $J=2$ perturbed by the quadrupole interaction (see Fig. 8a).

There are four other lines in the spectrum of $J=2$. They correspond to F changes of $7/2\rightarrow5/2$, $3/2\rightarrow1/2$, $7/2\rightarrow3/2$ and $5/2\rightarrow3/2$. Clearly, any one of these lines will be observed if the number of molecules in the "2, 0 state," which have resulted from non-adiabatic transitions from the "2, ±2 state," is either increased or decreased when an rf field of frequency equal to the frequency of the line is turned on. Whether an increase or decrease, or even a net "flop" of zero, results will depend on the quantitative aspects of the non-adiabatic interfield transitions about which nothing can be stated for a field as complicated as that which exists in the interfield regions of this apparatus. Line D is observed as an increase of the refocused beam; i.e., molecules in the "2, ±2 state" are "flopped into" the "2, 0 state" (lines A, B and C which come from $J=1$ are also observed as an increase of refocused beam). The frequencies of the lines corresponding to the $7/2\rightarrow5/2$ and the $3/2\rightarrow1/2$ transitions coincide with that of line A. An inspection of Fig. 8a shows that the $5/2\rightarrow3/2$ transition cannot be observed since molecules in the "2, ±1 state" are stopped by the wire-stop. The $7/2\rightarrow3/2$ transition could be observed (see Fig. 8a); however since it is not observed in the experiment it must be assumed that the quantitative aspects of the non-adiabatic transitions between the interfield regions are such as to make its intensity weak or even zero.

Table II summarizes the quadrupole interactions determined from the weak field data and compares them with those determined from the moderately strong field data. Within experimental error they agree very well. No difference is found between the quadrupole interaction for $J=1$ and $J=2$.

Finally, interactions of the type[2,5–8,10,11] $\mathbf{I}_1\cdot\mathbf{J}$ and $\mathbf{I}_2\cdot\mathbf{J}$ where $\mathbf{I}_1$ and $\mathbf{I}_2$ are the angular momenta of the K^{39} and the F nuclei, respectively, were not observed. The effect of $\mathbf{I}_1\cdot\mathbf{J}$ is to shift the lines, of $\mathbf{I}_2\cdot\mathbf{J}$ to split them. The $\mathbf{I}\cdot\mathbf{J}$ interactions are very weak compared to the quadrupole interactions. They are best observed at weak fields because at weak fields the resolution is best since the effect of the field on the broadening of the lines is eliminated.

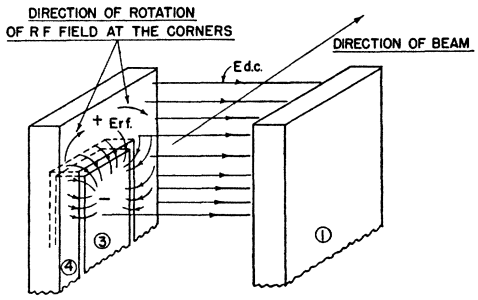

FIG. 10. Schematic perspective diagram of the C-field. 3 and 4 are at the same dc potential. The static homogeneous field, E_{dc}, is between 1 and 3, 4; the oscillating field, E_{rf}, is between 3 and 4. At the instant for which the diagram is drawn, 3 is charged negative, 4 is charged positive. With respect to a molecule moving in the direction of the beam, the oscillating field at the corners rotates in the direction shown. This direction is independent of the relative sign of 3 and 4.

Value of J

The spectrum shown in Fig. 4 was identified as coming from molecules in $J=1$ by the uniqueness of the hyperfine structure; i.e., the spectra obtained from $(J, m_J)\rightarrow(J, m_J')$ transitions of $(2,\pm1)\rightarrow(2,\pm2)$, $(2,\pm1)\rightarrow(2,0)$ or $(2,0)\rightarrow(2,\pm2)$ differ from the spectrum for a $(1,0)\rightarrow(1,\pm1)$ transition (compare Fig. 2b and 8b, c, d).

At weak fields lines A, B and C were assigned to the hyperfine structure resulting from the splitting of $J=1$ because the frequency ratios of these lines determine them uniquely as coming from that state. In addition, the values of the quadrupole interactions calculated from the weak field data for $J=1$ agree with those calculated from the moderately strong field data which has already been proved to come from the rotational state $J=1$.

V. THE DIPOLE MOMENT AND MOMENT OF INERTIA

When the $\boldsymbol{\mu}\cdot\mathbf{E}$ interaction is much larger than the quadrupole interaction, the splitting of the unperturbed Stark line is independent of the electric field, except for the mixing of the J states. However, when the electric field is large the energy of the molecule contributed by the $\boldsymbol{\mu}\cdot\mathbf{E}$ interaction is no longer proportional to E^2. W. E. Lamb, Jr., has calculated the exact solution of the Schrödinger equation for a linear diatomic molecule in an electric field. His solutions yield a three-term recursion formula. The energy eigenvalues are determined through the continued fraction method.[18] The analytical expression for the energy does not lend itself to the determination of μ and A. However, Hughes has fitted a polynomial[19] to Lamb's exact solution. He finds that for a $(1,0)\rightarrow(1,\pm1)$ transition the dimensionless formula:

$$\Delta W_{(1,0\rightarrow1,\pm1)}=0.15\lambda^2-0.010768\lambda^4+0.00125\lambda^6 \quad (2)$$

fits Lamb's exact solution for λ in the range 0 to 1.0.

The transition frequency is

$$\Delta\nu_{(1,0\rightarrow1,\pm1)}=\alpha E^2-\beta E^4+\gamma E^6 \quad (3)$$

where

$$\alpha=\frac{0.15}{h}\times\frac{\mu^2}{(\hbar^2/2A)},\quad \beta=\frac{0.010768}{h}\times\frac{\mu^4}{(\hbar^2/2A)^3},$$

$$\gamma=\frac{0.00125}{h}\times\frac{\mu^6}{(\hbar^2/2A)^5}.$$

The dipole moment and moment of inertia were determined by the following procedure. The frequency of line 1 defined in Fig. 2a was measured in the zeroth vibrational state at fields for which the λ^4 term of Eq. (2) is appreciable for three different fields corresponding to λ's of 0.38, 0.44, 0.49. From the theory of the hyperfine structure due to the quadrupole interaction, the frequency of the unperturbed Stark line was calculated. The effect of the mixing of J states on the frequency of line 1 is only 1 part in 15,000 of the frequency determined by the E^2 term of Eq. (3), and can be neglected in calculating the frequency of the unperturbed Stark line. Three simultaneous equations of the type of Eq. (3) yield α and β. From α and β

$$A=\frac{(0.15)^2}{0.0010768}\times\frac{h}{8\pi}\times\frac{\beta}{\alpha^2}(\text{g-cm}^2), \quad (4)$$

$$\mu^2=\frac{0.010768}{(0.15)^3}\times h^2\times\frac{\alpha^3}{\beta}(\text{e.s.u.})^2, \quad (5)$$

when E is expressed[20] in e.s.u. in Eq. (3).

[18] Reference 1, p. 620.
[19] H. K. Hughes, Phys. Rev. **76**, 1675 (1949).
[20] The field was measured in international volts/cm. E, however, is expressed in absolute units. The conversion factor is 1 international volt = 1.00034 absolute volts (Circular C 459, National Bureau of Standards, 1947). 1 e.s.u. = 299.796 absolute volts was also used.

TABLE III. Quadrupole interaction constants eqQ/h of the alkali-fluorides.

Molecule	Method	$\frac{eqQ}{h}$ Mc/sec.	Remarks
CsF[a]	Electric resonance	+ 1.240	vibrational states not resolved
$Rb^{85}F$[b]	Electric resonance	−70.312	zeroth vibrational state
$Rb^{87}F$[b]	Electric resonance	−34.000	zeroth vibrational state
$K^{39}F$	Electric resonance	− 7.938	zeroth vibrational state
NaF[c]	Magnetic resonance	8.512	sign not determined
Li^7F[d]	Magnetic resonance	0.408	sign not determined

[a] Reference 2.
[b] See reference 8.
[c] Private communication by D. Bolef and H. Zeiger.
[d] P. Kusch, Phys. Rev. **75**, 887 (1949).

Inserting the values of α and β in Eqs. (4) and (5), we obtain, for the zeroth vibrational state:

$A=(138.4\pm6.9)\times10^{-40}$ g-cm^2, $\mu=(7.33\pm0.24)$ Debye.

A Debye is 10^{-18} e.s.u. From the value of A the internuclear distance for $K^{39}F$ in the zeroth vibrational state is calculated to be (2.55 ± 0.06) angströms. The experimental errors are mainly due to the non-uniformity of the C-field. It was not possible to measure μ and A for the other vibrational states because their lines are not resolved at these high fields.

VI. THE MILLMAN EFFECT

Figure 9 shows the data taken for the determination of μ and A at $\lambda=0.38$. These lines are identified in Fig. 2. Each of the lines has two side peaks. It will now be shown that the side peaks are caused by the Millman[21] effect. The C-field is sketched in Fig. 10. The components are labeled to correspond to the labels of Fig. 2, reference 2, where the C-field is discussed in detail. The homogeneous static field is between plates 1 and plates 3, 4. Plates 3 and 4 are coplanar and at the same d.c. potential. The r-f field is superposed on the static field by connecting the output of a vacuum tube oscillator between 3 and 4. The lateral position of the beam is approximately midway between 1 and 3, 4. Its vertical position is such that its height (5 mm) is bisected by the horizontal boundary between 3 and 4. At the corners the direction of the field changes (see-Fig. 10). With respect to a moving molecule the r-f field is linearly polarized only in the region between the corners. At the corners it is a superposition of oscillation and rotation. It is clear that the rotation takes place in the same direction during each half-period of the oscillation. The direction of rotation is indicated in Fig. 10 when 3 is negative and 4 is positive. If the linearly polarized oscillating field is resolved into two circularly polarized components, one rotating in the

[21] S. Millman, Phys. Rev. **55**, 628 (1939).

same direction as the rotation at the corners, the other rotating in the opposite sense, we will have two frequencies at the corners, $\nu+\Delta\nu$ and $\nu-\Delta\nu$. Here ν is the applied oscillator frequency, and $\Delta\nu$ is the effective frequency of rotation of the linearly polarized field which the moving molecule sees at the corners. It is shown in the Appendix that the dipole matrix elements of both circularly polarized components are non-vanishing for a polar molecule in an electric field. Therefore if the oscillator frequency is fixed and the field is varied, which is the case for the data shown in Fig. 9, three lines will appear: two side peaks due to circularly polarized fields of frequency $\nu+\Delta\nu$ and $\nu-\Delta\nu$ at the corners, and a central peak due to each circularly polarized component of frequency at the central portion of 3 between the two corners. Only one side peak[21] is observed in the magnetic resonance data because only one circularly polarized component of the rf field gives a non-vanishing dipole matrix element.

The separation of a side peak from the central peak gives $\Delta\nu=160$ kc/sec. for $K^{39}F$. From the most probable molecular velocity in the beam the distance over which the rotation at a corner takes place is calculated to be 0.3 cm. Since plates 3 and 4 are separated by a distance of 0.04 cm, this seems a reasonable value. The total length of the C-field is 6 cm, the length of 3 (along the beam) is 4 cm.

VII. DISCUSSION

Table III gives the quadrupole interactions of all the alkali-fluorides measured to date. It is complete except for $K^{41}F$ and $Li^{6}F$. This table can tell little until the important problem of separating q and Q is solved. The value of q can be calculated if the molecular wave function is known.

It is probable that there is a variation of the quadrupole interaction with vibrational state in all the alkali fluorides of the same order of magnitude as that found[8] for $K^{39}F$, $Rb^{85}F$ and $Rb^{87}F$, namely, $\sim$1 percent when the vibrational quantum number increases by unity. The magnitude of this variation would be too small to be observed in CsF or $Li^{7}F$. Indeed, it was not observed in the electric resonance spectrum[2] of CsF.

If the sign of q is assumed to be identical for the alkali-fluorides, then the sign of the electric quadrupole moment of the K^{39}, Rb^{85} and Rb^{87} nuclei is opposite to that of the Cs nucleus.

The internuclear distance $r=2.55$A for $K^{39}F$ is of interest when viewed in the light of Trischka's experiment. For CsF, Trischka[3] found that the internuclear distance is 6 percent smaller than that of CsH[1]. For $K^{39}F$ the internuclear distance in the zeroth vibrational state is 12 percent larger than that[22,23] of $K^{39}H$[1]. Further, the internuclear distance of $K^{39}F$ is larger than that of CsF (2.34A); the internuclear distance of all the other potassium halides, however, is smaller than that of the corresponding cesium halide.[24]

We would like to express our gratitude to Professor I. I. Rabi for his continued interest and for many clarifying discussions. We would also like to thank Professor J. W. Trischka, who began this research with one of us, and S. Miller, who helped in the laboratory.

APPENDIX

The probability amplitudes of the energy eigenfunctions are related by the equation

$$i\hbar\dot{a}_k(t)=\Sigma_n a_n(t)[k|H'|n]\exp[-(i/\hbar)(E_n-E_k)t]. \quad (6)$$

H' is the interaction of the system with the oscillating field. Let $\omega_{kn}=E_k-E_n/\hbar$ and assume that at $t=0$, $a_j(0)=1$; then

$$i\hbar\dot{a}_k(t)=(k|H'|j)\exp(i\omega_k t). \quad (7)$$

The linearly polarized oscillation:

$$E_x=4E_0^x\cos\omega t=2E_0^x[\exp(+i\omega t)-\exp(-i\omega t)] \quad (8)$$

can be replaced by the sum of the left-circularly polarized oscillation

$$E_L=\mathbf{i}E_0^x[\exp(+i\omega t)+\exp(-i\omega t) -\mathbf{j}iE_0^y[\exp(+i\omega t)-\exp(-i\omega t)] \quad (9)$$

and the right-circularly polarized oscillation

$$E_R=\mathbf{i}E_0^x[\exp(+i\omega t)+\exp(-i\omega t)] +\mathbf{j}iE_0^y[\exp(+i\omega t)-\exp(-i\omega t)]. \quad (10)$$

In (9) and (10) $E_0^x=E_0^y$. Since $H'=-\mathbf{p}\cdot\mathbf{E}=-(p_xE_x+p_yE_y)$, where $\mathbf{p}$ is the electric dipole moment of the system, (7) becomes

$$\begin{aligned}-i\hbar\dot{a}_k(t)=&E_0^x\{\exp[+i(\omega_{kj}+\omega)t+\exp[-i(\omega_{kj}-\omega)t]\}(k|p_x|j)\\ &-iE_0^y\{\exp[+i(\omega_{kj}+\omega)t-\exp[-i(\omega_{kj}-\omega)t]\}(k|p_y|j)\\ &+E_0^z\{\exp[+i(\omega_{kj}+\omega)t+\exp[-i(\omega_{kj}-\omega)t]\}(k|p_x|j)\\ &-iE_0^y\{\exp[+i(\omega_{kj}+\omega)t+\exp[-i(\omega_{kj}-\omega)t]\}(k|p_y|j). \quad (11)\end{aligned}$$

The sum of the first two terms on the right of (11) represent the matrix element of the left-circularly polarized component, the sum of the third and fourth terms that of the right-circularly polarized component. Now[25]

$$\pm i(m|p_x|m+1)=(m|p_y|m\pm1). \quad (12)$$

If the transition involves $m\rightarrow m+1$, Eqs. (11) and (12) show that only the left-circularly polarized component has a non-vanishing matrix element. Similarly, when $m\rightarrow m-1$, only the right-circularly polarized component has a non-vanishing matrix element. Since the energy of a diatomic molecule in an electric field is degenerate with respect to $+m$ and $-m$, both matrix elements are non-vanishing.

[22] T. Hori, Mem. Ryojun Coll. Eng. **6**, 1 (1933).
[23] M. Almy and C. D. House, Phys. Rev. **42**, 242 (1932).
[24] Maxwell, Hendricks, and Mosley, Phys. Rev. **52**, 968 (1937).
[25] E. U. Condon and G. H. Shortley, *Theory of Atomic Spectra* (Macmillan Company, Inc., New York, 1935), p. 63.